Summer 2021

Functionalized Ionic Liquids for Improved CO2 Hydrogenation Catalysts

Amol Nanduji Jaybhaye
Western Kentucky University, amolnanduji.jaybhaye728@topper.wku.edu

FUNCTIONALIZED IONIC LIQUIDS FOR IMPROVED CO_2 HYDROGENATION CATALYSTS

A Thesis
Presented to
The Faculty of the Department of Chemistry
Western Kentucky University
Bowling Green, Kentucky

In Partial Fulfillment
Of the Requirements for the Degree
Master of Science

By
Amol Nanduji Jaybhaye

August 2021

FUNCTIONALIZED IONIC LIQUIDS FOR IMPROVED CO_2 HYDROGENATION CATALYSTS

Date Recommended 06/21/2021

Lawrence Hill Digitally signed by Lawrence Hill Date: 2021.07.07 17:43:43 -05'00'

Dr. Lawrence J. Hill, Director of Thesis

Kevin Williams Digitally signed by Kevin Williams Date: 2021.07.08 08:13:38 -05'00'

Dr. Kevin Williams

Bangbo Yan Digitally signed by Bangbo Yan Date: 2021.07.06 16:32:32 -05'00'

Dr. Bangbo Yan

Associate Provost for Research and Graduate Education

I dedicate my thesis to few important persons of my life,

My beloved grandfather, the late Mr. Arjun Tatyobha Doifode, helped us in hard times and always pushed us for big dreams. I hope you must be smiling and showering love on us from heaven. We miss you, BABA.

My parents Mrs. Lata and Mr. Nanduji Laxman Jaybhaye, who worked so hard for me and taught me to dream big and fight for it.

My elder brother cum best friend Vinod Nanduji Jaybhaye is always there for me, my ray of hope.

Lastly, the person I know for a decade, my dearest friend Nitin Tanaji Katare, I will always be thankful for your help and faith in me.

ACKNOWLEDGMENTS

Foremost, I would like to pay my deepest thanks to my research advisor Dr. Lawrence Hill, for offering me an opportunity to work in his laboratory. I am fortunate to work under him and will always be thankful for nurturing me. He always enthusiastically helps me with all my questions, starting from digital calendar management, searching research articles, formal writing, and presentation skills. I learn a lot from him personally and professionally. I still remembered when he spoiled his weekends for me and was present for me. Lastly, Iwould also like to thank him for timing flexibility for the research lab, which is why Ihave been able to complete all my tasks as a student and teaching assistant in the department. I could not imagine having a better mentor for my research thesis than Dr. Hill. My sincere thanks go to the committee members Dr. Kevin Williams and Dr. Bangbo Yan. I am grateful for the time and efforts they have taken to be on my thesis defense committee. Thanks for your valuable help and feedback on my research.

I want to thank Dr. Stuart Burris, Former Department Head of Chemistry Department, and Graduate School, Western Kentucky University, for accepting me as a master's student and offer me a graduate assistantship throughout my program. I also want to thank Dr. Eric Conte for his help and care for international students. I also like to thank Haley Smith for always answering my queries with love and patience. I also appreciate Ms. Alicia Pesterfield and the stockroom team for providing chemicals even in this challenging time. I am immensely grateful to the Chemistry Department, the Graduate School, International student office, Indian student association (ISA), Western Kentucky University for their support and love.

I want to thank my research lab mates Augustine Yusuf, Jeffery Palmer and TA colleague Fox Buther, Christian Alcantar from WKU.

Moreover, I would like to express my gratitude to my family and friends for their endless support, especially all my roommates from the very beginning, Nitin Katare, Ajinkya Indulkar, Arpan Sheth, Aditya Golukonda, Dhruval Patel, and Viral Bhavsar, Dhruvin Patel, Kishan Patel, and Haly Patel for their consistent support. I would also like to thank my seniors Dr. Rahul Chilbule, Dr. Amit Pant and Dhiraj Bhagwat and all my friends from India who always have there for me.

Finally, I am grateful to my students who propelled me to improve my teaching abilities and helped me to pave my path for the coming future.

TABLE OF CONTENTS

LIST OF FIGURES AND SCHEMES

Figures **Page**

Schemes **Page**

FUNCTIONALIZED IONIC LIQUIDS FOR IMPROVED CO_2 HYDROGENATION CATALYST

Amol Nanduji Jaybhaye August 2021 39 Pages

Directed By: Dr. Lawrence Hill, Dr. Kevin Williams, and Dr. Bangbo Yan

Department of Chemistry Western Kentucky University

Climate change is one of the biggest problems we are facing today, and anthropogenic greenhouse gases contribute significantly to it. Among greenhouse gasses, carbon dioxide emission is increased drastically and affecting majorly for increasing global temperature, and anything we can do to mitigate carbon dioxide emission will be helpful. A carbon dioxide hydrogenation reaction is a promising technique that can convert carbon dioxide into value-added chemicals, but the reaction rate is slow, and for that, we can use catalysts that will accelerate the reaction rate. Platinum-based nanoparticles have sparked research related to energy and environmental catalysts. Catalytic properties are depending on physical and chemical parameters. Engineering the shape and surface structure of platinum nanocrystals effectively optimizes their catalytic activities toward various reactions. These complex shapes are generally achieved using traditional ligands, which cause crystals to grow preferentially in certain directions by binding to other facets and limiting their growth. We can use the mixtures of functionalized ionic liquids to replicate traditional solvents and ligands' nucleation and growth environments. In this way, platinum nanoparticles can be synthesized using ionic liquids to facilitate the carbon dioxide hydrogenation reaction.

Chapter 1: Introduction

1.1 Carbon dioxide (CO_2) emission

Climate change is one of the biggest problems we are facing today, and anthropogenic greenhouse gases contribute significantly to it. These greenhouse gas emissions occur primarily by burning fossil fuels. Carbon dioxide is one of the major greenhouse gases, and increases in carbon dioxide levels are causing the rise in global temperature, leading to unexpected changes in the atmosphere, rain cycle, ecosystems, natural habitat, and increased sea level.[1] We can see drastic growth in CO_2 emission to the date and projections as shown in Figure 1.[2]

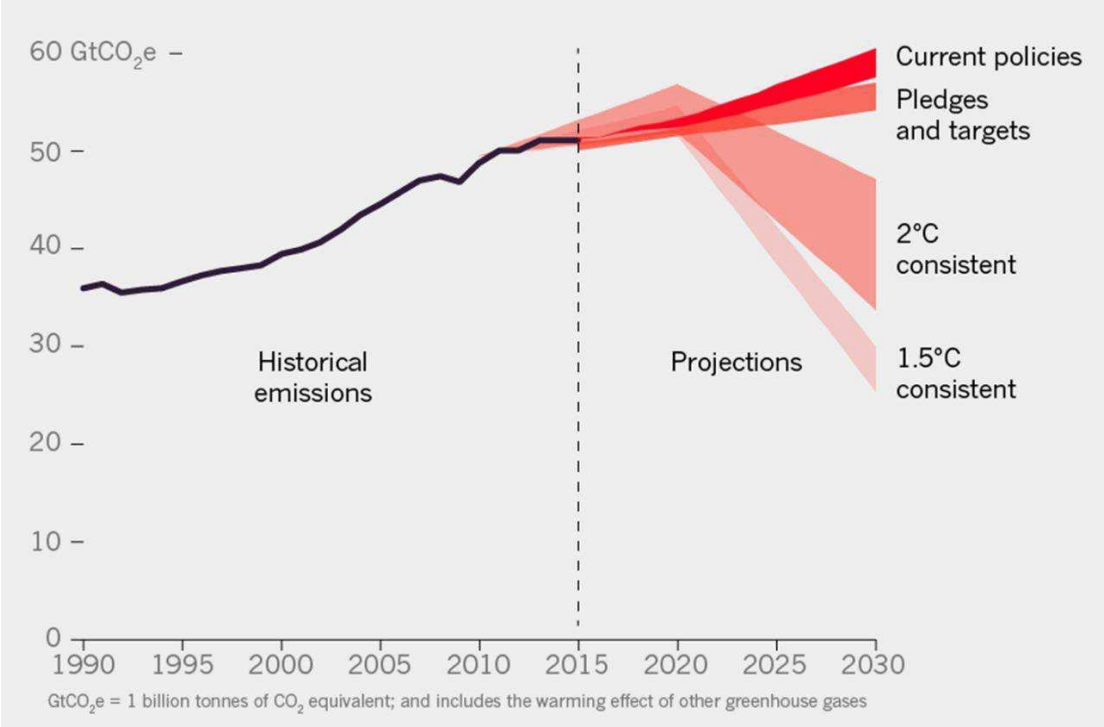

Figure 1: Historical emission data and projections for CO_2 emission. Figure reproduced from reference 2.

It was an emergency for nations to make policies and pledges to reduce CO_2 emissions to control increasing global temperature. For example, for the world to meet the Paris target

of limiting global warming to 1.5°C, nations would have to cut their CO_2 emissions to zero by 2050. Even staying below 2°C of warming would require massive cuts.[2] However, based on current pledges and targets made by nations globally, we are well above targeted temperatures. At current policies and pledge, the global temperature may rise by 4-5 degrees by 2030. Several strategies are used for reducing carbon dioxide concentration in the atmosphere, including capture, separation, storage, and utilization.[3] Utilization focuses on transforming carbon dioxide into value-added chemicals, and thus, carbon dioxide can be treated as cheap, renewable, and nontoxic C1 feedstock.

1.2 CO_2 hydrogenation reaction

CO_2 hydrogenation to produce various products via catalytic processes is a promising strategy. As a result, the catalytic combination of CO_2 and hydrogen reduce anthropogenic emissions into the Earth's atmosphere and produces carbon compounds used as fuel or precursors to produce various chemicals like formaldehyde, methanol, ethanol, and methane.[4,5] But it is challenging due to the thermal stability of CO_2, making reaction conversions low. Catalysts can be used to make this conversion fast and effective.[6]

1.3 Catalysts for CO_2 hydrogenation

Catalysts are crucial in every part of life, from creating chemicals and polymers to cleaning car emissions and wastewater treatment. Catalysts change the kinetics of a chemical reaction without being consumed, accelerate the rate of reaction, and modify the selectivity of a reaction, allowing for the increased production of desirable products by decreasing the activation energy.[7] There are two types of catalysts, homogeneous and heterogeneous. Homogeneous catalysts are in the same phase as the reactants, most commonly in the liquid phase. Heterogeneous catalysts frequently contain a solid, active metal phase dispersed on

a support and are used with gas or liquid reactants.[7] These catalysts can be used for the CO_2 hydrogenation reaction.[8] Carbonyl carbon on carbon dioxide is electron-deficient, and CO_2 has a strong affinity toward nucleophiles and electron-donating reagents, so we can hydrogenate CO_2 by two routes as shown below in Scheme 1.[9] In the first route, we can hydrogenate CO_2 in sequence to HCO_2H (Formic acid), formaldehyde, methanol and then methane. In the second route, CO_2 is converted to carbon monoxide (CO) via the reversed water gas shift reaction (RWGS) and further reduced yielding formaldehyde, methanol, and methane or eventually heavier hydrocarbons (HC)/oxygenates through the Fischer-Tropsch process, as shown in Scheme 1.

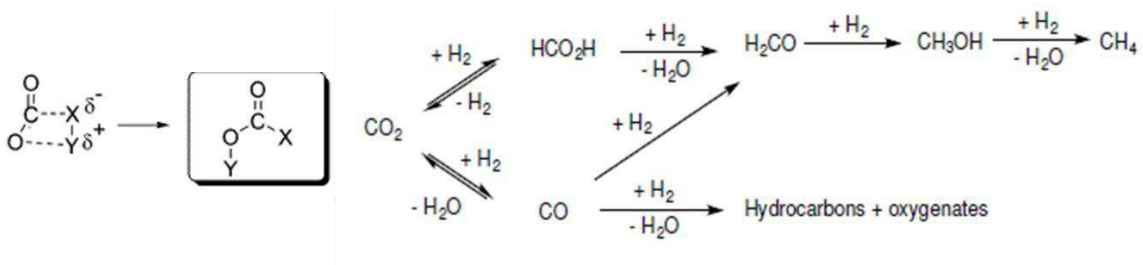

Scheme 1: Reaction pathways for CO_2 hydrogenation. Reproduced from reference 9.

Therefore, depending on thermodynamic/kinetic balances and particularly on the fine-tuning of catalysts' electronic and geometric properties, a series of chemicals and fuels can be produced from CO_2 hydrogenation either via the CO or formic acid pathways.[9] Qadir et al synthesized ferromagnetic ruthenium-iron (RuFe) nanoparticles in ionic liquids (ILs) and used them for selective hydrogenation of CO_2 into formic acid or hydrocarbons (HC).[9] The distinct CO_2 hydrogenation pathways (HCO_2H or FT via RWGS) catalyzed by the RuFe alloy are directly related to the nature of the IL anion, the support, and the metal alloy. ILs form a cage around NPs, providing an ionic nano-container environment that

allows control of the diffusion of reactants, intermediates, and products (mainly via hydrophobicity and contact ion pairs) to the active catalytic sites. In this way, Qadir et al focused on synthesizing heterogeneous catalyst with hydrophobic anion that will favor carbon monoxide pathway producing long-chain hydrocarbons[9] and showed how nanoparticles and ionic liquids could be used in catalysts to speed up chemical reactions and reduces the number of catalytic materials required to achieve the desired results, saving money and reducing pollution.[10]

1.4 An overview of nanotechnologies and nanoparticles

Nanotechnology as a field of research was introduced in the last century, and the word Nano is a prefix used to describe ‘one billionth of something.’ It first came into consideration after a presentation on nanotechnology by Nobel laureate Richard P. Feynman in 1959 in his famous lecture "There's Plenty of Room at the Bottom: An Invitation to Enter a New Field of Physics".[11] Since then, many revolutionary advances in chemistry, physics, and biology have demonstrated Feynman's ideas about manipulating matter at the atomic scale. Norio Taniguchi coined the term "nanotechnology" in 1974 to describe extra-high precision and ultra-fine dimensions.[12] By predicting improvements and miniaturization in integrated circuits, optoelectronic devices, mechanical devices, and computer memory devices, he pioneered the “top-down approach.” K Eric Drexler introduced the “bottom-up approach” ten years later when he discussed creating larger objects from their atomic and molecular components.[13] Every substance, regardless of its composition, exhibits new properties when the size is reduced to the nanoscale. The factors that govern larger systems do not necessarily apply at the nanoscale. Because nanomaterials have larger surface areas, phenomena like friction were more critical than

larger systems.[14] Nanoparticles (NPs) can be classified into different groups based on various criteria. NPs can be categorized according to their dimensionality, morphology, chemical composition, and physical composition.[15] Based on composition and electronic properties, NPs are classified as metal NPs, ceramic NPs, semiconductor NPs, carbon-based NPs, polymeric NPs, and lipid-based NPs. There is ample research on metal nanoparticles like gold, silver, platinum, and palladium due to unusual chemical, optical, and electrical properties compared to bulk materials. For example, gold NPs can be synthesized and prepared using a combination of sonoelectrochemical and ultrasonic vibration.[16] The size, shape, and activated surface area of metal NPs are crucial for several applications such as catalysis and adsorption processes.[10]

1.5 General aspects of nanoparticle growth

The shape of nanoparticles can be tuned by suitably controlling the experimental parameters like concentration of the metal precursor, reducing agents, stabilizer, and reaction conditions such as temperature and time. Various methods are used to synthesize nanoparticles, and thus they are broadly divided into two main classes, bottom-up and top-down approaches.[14] A top-down synthesis is a destructive approach in which larger objects are used as starting material and converted into smaller units and eventually into suitable NPs. On the other hand, the bottom-up approach or building-up approach is precisely opposite of the top-down approach in which smaller units are combined and are converted into suitable NPs.[14]

We can synthesize noble metal nanostructures, as shown in Figure 3, in which noble atoms nucleate and form clusters (fluctuating structures).[17] Once the nuclei attain a specific size, they become seeds: either a single-crystal, singly twinned, or multiply twinned particle.

Depending on how crystals are formed, we get different atoms presented to surfaces called facets. We can get different shapes based on the facets exposed, shown in Figure 2, where the colors green, orange, and purple colors represent the (100), (111), and (110) facets, respectively. The parameter R is the ratio between the growth rates and the (100) and (111) directions. Most metal nuclei incorporate twin boundary defects that enable lower surface energy.

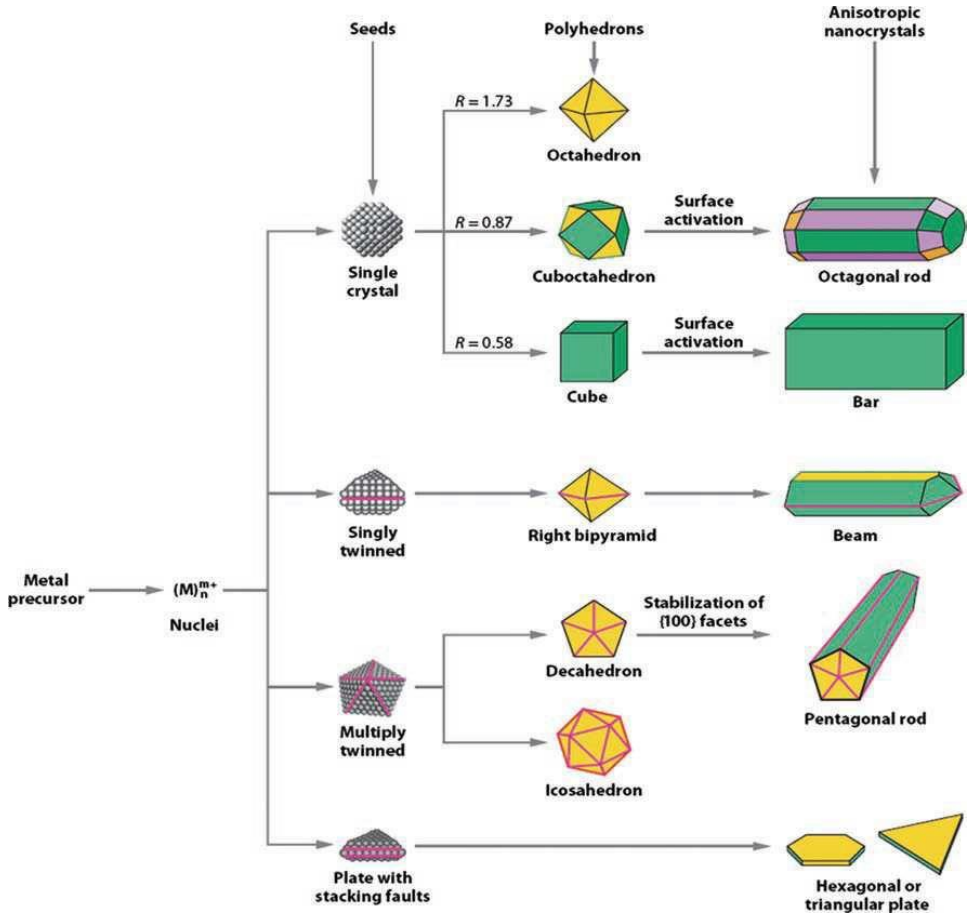

Figure 2: Schematic illustrating various stages of the reaction leads to forming noble-metal nanoparticles with different shapes. Reproduced from reference 17.

As the growth proceeds, changes in the defect structure of the nuclei become too costly relative to the available thermal energy, and they become trapped in the given morphology. This process results in various kinds of seeds such as multiply twinned, singly twinned,

and single-crystal seeds, with fivefold symmetry and converted into polyhedrons and eventually in anisotropic nanoparticles.[17,18] In this way, we can control the facet's growth and get different anisotropic nanoparticles.

1.6 Morphologically controlled platinum NPs and alloys

Metal NPs received particular attention as catalysts due to their electronic, chemical, and optical properties. Metal NPs showed high catalytic activities even under mild conditions as they favor the interaction between the reactants and the surface of the catalysts compared to other nanocatalysts.[19] Among all metal NPs, platinum nanoparticles exhibited excellent catalytic activity. It has an unfilled 5d shell electron orbital with a rich electronic structure and shows catalytic activities in many fields, including automobile, exhaust gas treatment, fuel cell, petroleum refining, organic synthesis, and hydrogen production. Controlling the shape of platinum nanoparticles (PtNPs) can be used as a model system to get facet-dependent activity known as geometric effects. It has been demonstrated that the catalytic performance (both activity and selectivity) of platinum nanoparticles strongly depends on the shape, which is demonstrated by computational and experimental studies.[20] It is seen that chemical activity and property depend on the atomic arrangement of the platinum surface. Atomic arrangement successively will regulate sorption energies and geometries of substrate molecules and intermediates throughout a molecular transformation.[21] It is noteworthy that geometric effects are vital in nanocatalysis and are favored by the presence of steps, kinks, and atoms with low coordination numbers relative to atoms with high coordination numbers.[22] One can have prominent catalytic activity by controlling the physicochemical properties of platinum nanoparticles. Platinum-based nanomaterials

showed a plethora of chemical transformations dependent on physicochemical properties, as shown in Table 1.

Shape	Size(nm)	Molecular Transformation	Ref
Spherical	3.7 ± 0.7	Oxidation of hydrazine	23
Multioctahedra	40 ± 4	Reduction of oxygen	24
Cubic	12.3 ± 1.4	Hydrogenation of benzene	23
Cuboctahedra	13.5 ± 1.5	Hydrogenation of benzene	23
Cubes	13	Hydrogenation of carbon dioxide	25
Octapods	8	Hydrogenation of carbon dioxide	25

Table 1. Summary of few platinum nanocatalysts towards chemical transformations.

In the above table, Khan et al synthesized platinum-cobalt alloy (Pt_3Co) cubes and octapods system with oleylamine and octanethiol ligands.[25] They found that catalytic performance of Pt and Pt_3Co particles are highly shape-dependent due to charge accumulation at tips and vertices, as shown in Figure 3.

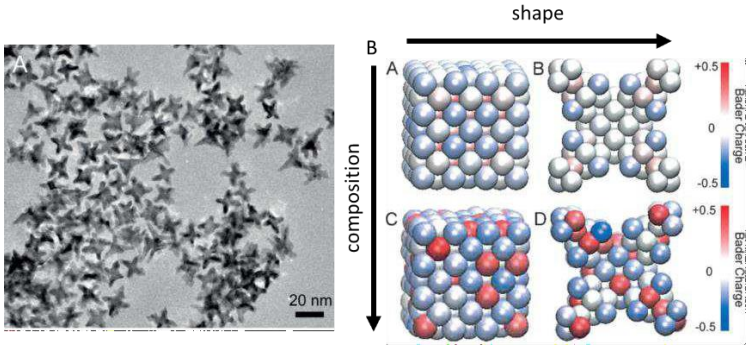

Figure 3: A) TEM images of the Pt_3Co octopods, B) Controlled nanoparticle shape affects available facets and charge distribution at the particle surface. Figure adapted from reference 25.

Platinum cobalt particles outperformed the pure platinum particles due to electronegativity differences between platinum and cobalt, resulting in more charge separation. In the above system (Figure 3), the hydrogenation of CO_2 relies on the accumulation of negative charge on the nanoparticle surface, which will be strongly dependent on surface charges.

1.7 Ionic liquids to control both nanoparticle shape and CO_2 hydrogenation products

Here, we seek to combine the benefits of nanoparticle shape control using ionic liquids to favor CO_2 hydrogenation products. Our system is based on the work of Khan et al, who used amines and thiols in an inert solvent to synthesize highly branched Pt and Pt_3Co nanoparticles.[25] We, therefore, target the synthesis of ionic liquids with amine and thiol functional groups to allow for shape-controlled nanoparticle synthesis (Scheme 2). Imidazolium ionic liquids (amine and thiol) with hydrophobic Tf_2N anions were chosen to allow for selective hydrogenation of CO_2 into formic acid or hydrocarbons (HC).[9] Amine and thiol functionalized ionic liquids are expected to facilitate the formation of high-index facets and form a cage around NPs, providing an ionic nano-container environment that allows improved catalytic activity and helps convert CO_2 into valuable chemical products.[9]

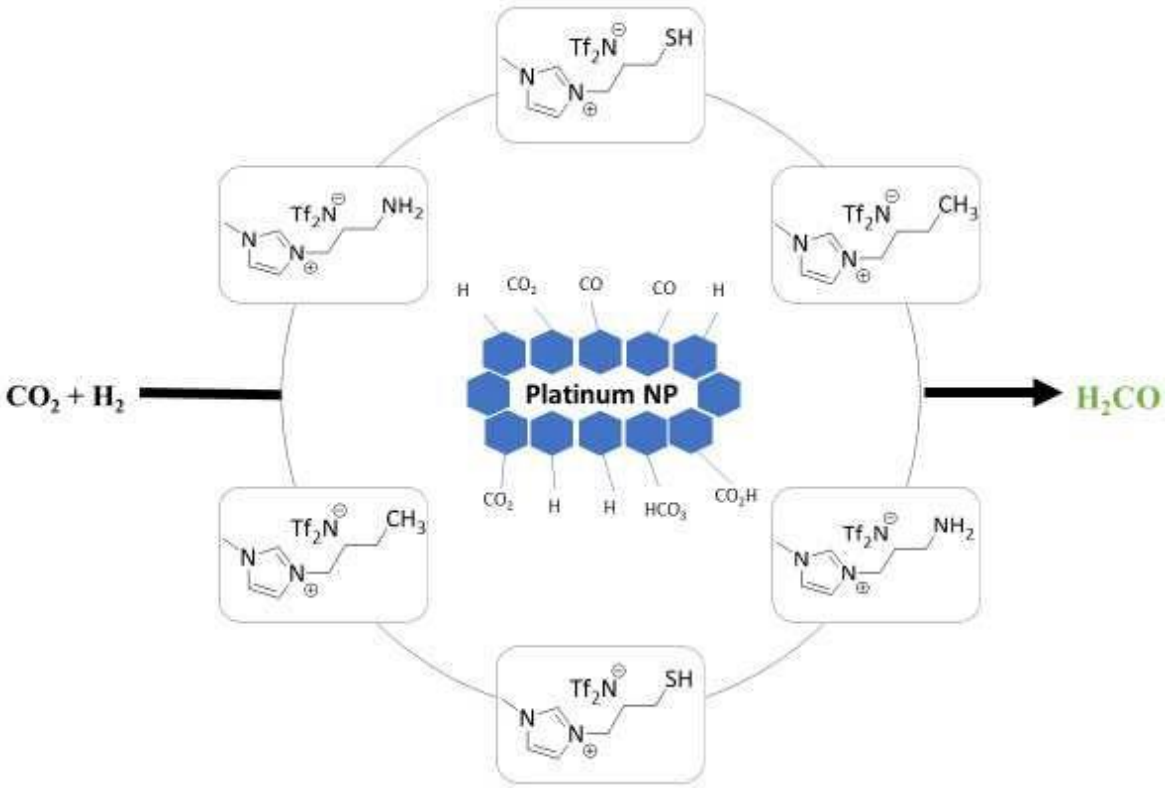

Scheme 2: A cartoon representation showing functionalized imidazolium ionic liquids and platinum nanoparticles for hydrogenation of CO_2.

The remaining chapters of this thesis cover the synthesis of amine-functionalized ionic liquids (Chapter 2) and thiol-functionalized ionic liquids (Chapter 3), followed by a conclusion and future directions (Chapter 4).

Chapter 2 - Synthesis of amine-functionalized ionic liquids

The amine-functionalized imidazolium ionic liquid was synthesized in two steps based on a previously reported method, as shown in Figure 4. In the first step, 1-methylimidazole was quaternized by reacting with the hydrogen bromide salt of 3-bromopropylamine to form the amine-functionalized ionic liquid with a bromide anion, compound 1. The targeted ionic liquid, compound 2, was synthesized by reacting with lithium bis(trifluoromethanesulfonyl)imide ($LiTf_2N$).

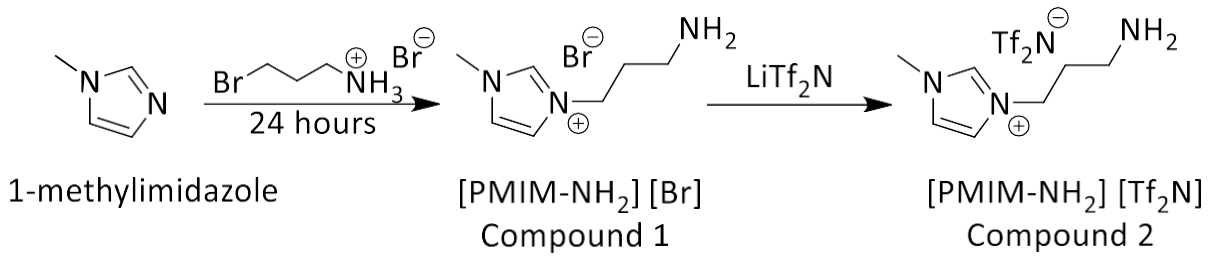

Figure 4: Reaction scheme for synthesizing amine-functionalized imidazolium ionic liquid [PMIM-NH_2] [Tf_2N], Compound 2.

2.1 Materials and Instrumentation

1-methylimidazole was purchased from Arcos Organics, 3-bromopropylamine hydrobromide, sodium hydroxide (NaOH), lithium bis(trifluoromethanesulfonyl)imide ($LiTf_2N$) were purchased from Tokyo Chemical Industry. Tetrahydrofuran (THF), dichloromethane (DCM), diethyl ether, ethyl acetate purchased from Sigma Aldrich. Deuterated dimethyl sulfoxide (DMSO-d6) was purchased from Oakwood Chemical. Deuterated water (D_2O) was purchased from Aldrich Chemistry. All the chemicals were used directly with no further purification. A JNM-ECZS 400 MHz nuclear magnetic resonance instrument (JEOL) was used to characterize the synthesized products, and NMR data were processed using MestReNova software.

2.2 Small scale synthesis of compound 1 [PMIM-NH_2] [Br]

A modified version of the reaction described by Bates et al was used to create the desired ionic liquid at a small scale with an amine functional group.[26] The first step of synthesis was the quaternization reaction in which 1-methylimidazole reacted with 3-bromopropylamine hydrobromide, as shown in Figure 5. In this quaternization reaction, the lone pair on the nitrogen atom from 1-methylimidazole attacked the alpha carbon of 3-bromopropylamine in a nucleophilic substitution reaction (S_N2) with bromide acting as leaving group and gave compound 1 that is propyl methyl imidazolium bromide with bromide anion abbreviated as [PMIM-NH_2] [Br].

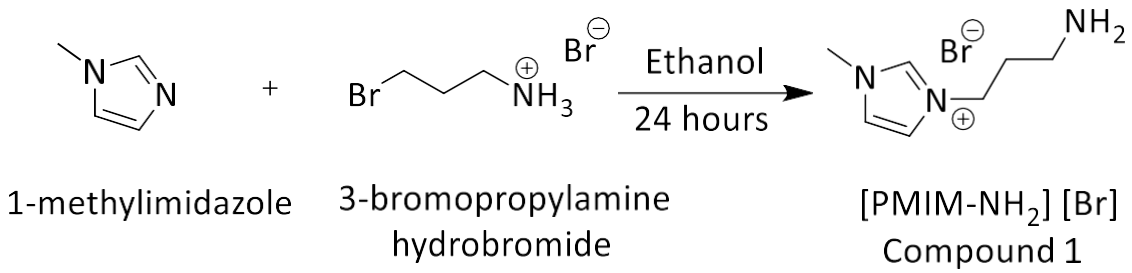

Figure 5: Reaction scheme for the small-scale synthesis of amine-functionalized imidazolium ionic liquid with the solvent, Compound 1.

For the synthesis, 1-methylimidazole (3.99 mL, 50 mmol) and 3-bromopropylamine hydrobromide (10.99 g, 50 mmol) were added to a 100 mL round bottom flask dissolved in 25 mL ethanol with a stir bar, refluxed for 24 hours with an oil bath having a temperature of 100 °C and stirred at 300 rpm. Ethanol was removed under reduced pressure by a rotary evaporator to give a residue. This residue was dissolved in (40 mL) water and evaporated under reduced pressure leaving a yellow-brown colored product. It was washed twice with a 1:1 mixture of tetrahydrofuran and ethanol (40 mL each wash). The residue was dried under a vacuum oven at 70 °C for 22 hours, leaving a viscous yellow oil. Proton nuclear

magnetic resonance spectroscopy (^{1}H-NMR) was used for the characterization of compound 1.

- **2.2.1. Results and Analysis**

Firstly, we used deuterated dimethyl sulfoxide as an NMR solvent to ensure we get all the expected eight signals from our compound 1. If we use deuterated water as an NMR solvent and exchangeable protons in the compound, then exchangeable protons from the structure will not show up on the spectrum. ^{1}H-NMR (DMSO-d6) spectroscopy of the crude product provided evidence for the formation of compound 1 (Figure 6).

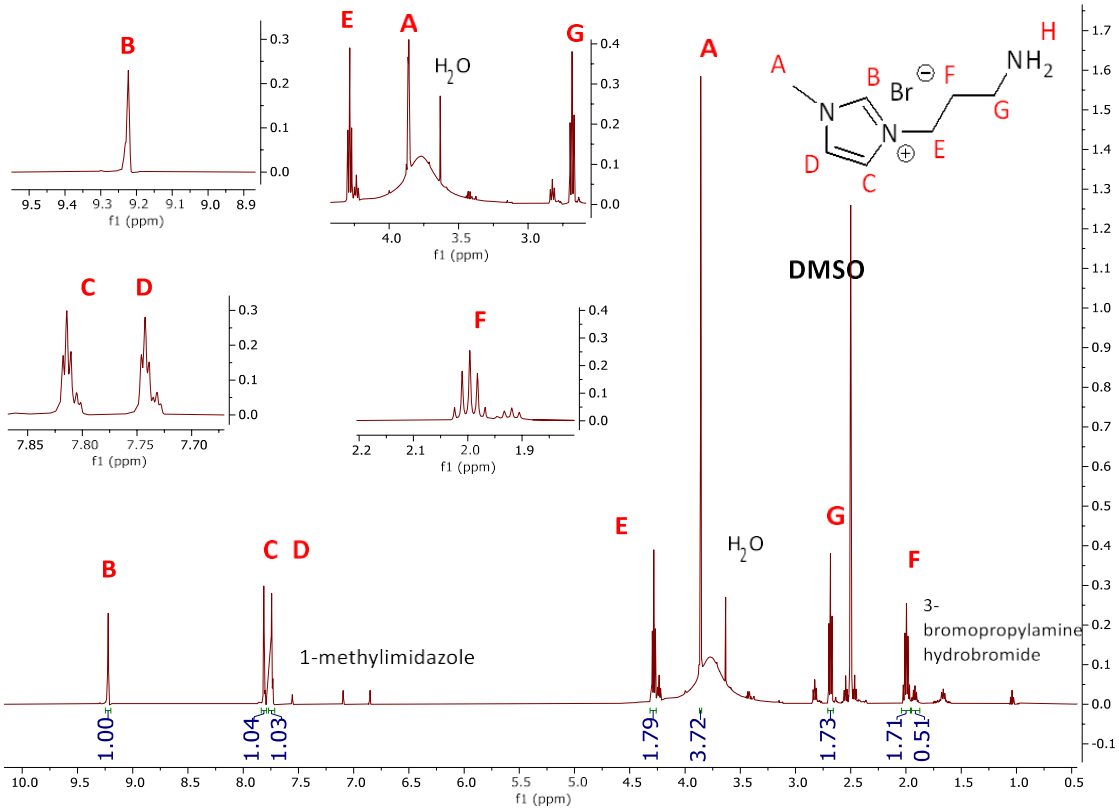

Figure 6: ^{1}H-NMR (DMSO-d6) spectrum and the structure of compound 1 [PMIM-NH_2] [Br] before further purification

We found three signals assigned to aromatic protons in the range of 7 – 10 ppm in the NMR spectrum in which proton B was found to be singlet, as shown in figure 6, along with insects

for every proton. Protons C and D were found to be doublets with an integration value of approximately one each. Adjacent to aromatic protons, we can see three other small signals with a similar pattern and similar relative integration values attributed to residual 1-methylimidazole not removed from the actual mixture. The aromatic signals from compound 1 and aromatic signals from starting material (1-methylimidazole) in the spectrum gave us the confidence that these two signals are from different molecules and synthesized a new product. Then the next diagnostic proton for the product (compound 1) would be proton A, and it is expected to be a singlet with a large integration value of approximately three. On the spectrum, we got a singlet that integrates higher than three. Furthermore, we attribute the higher integration value of proton A to an unknown broad peak at 3.8 ppm contributing to the integration value which overlaps with peak A. We found alkyl protons E, F, and G in the region 2-5 ppm, and protons E and G showed triplet on the spectrum and proton F with proper multiplet (pentet) and all protons having approximate integration of two. We were still missing proton H, and it may be buried in the broad peak around 3.7 ppm. To ensure this, we need to perform some experiments to purify the product and get the proper H signal. There were unexpected signals on the NMR spectrum. The unknown signals may be from starting materials 1-methylimidazole and 3-bromopropylamine hydrobromide. To find the unknown signals, we stack the NMR data of starting materials and compound 1. Based on the stack plot (Figure 7), the three signals in the range 6.5 - 7.5 ppm on the compound 1 spectrum are attributed to unreacted 1-methylimidazole. So, to get a product with less or no impurities, it was purified.

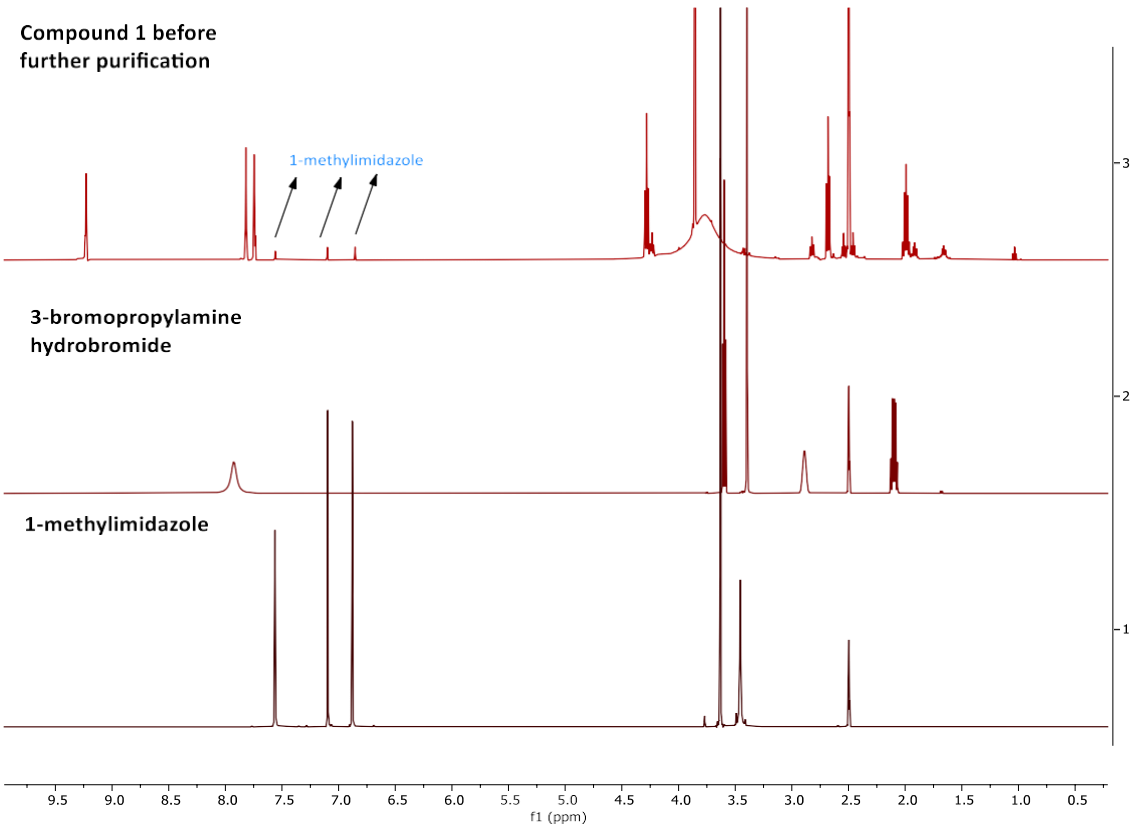

Figure 7: Stacked ^{1}H-NMR (DMSO-d6) spectra of starting materials and compound 1 before purification.

Compound 1 was purified to remove the unreacted starting materials. In the purification process, we added 30 mL of water to the solution, and sodium hydroxide was added to make pH 10. The organic-soluble species were extracted by dichloromethane (three extractions, 20 mL each), and water was evaporated, and the residue was washed three times with diethyl ether (50 mL each). The product was dried under a vacuum oven at 70 °C overnight for 25 hours, leaving the dark brown semi-translucent product. The ^{1}H-NMR spectrum of compound 1 after purification is shown in below Figure 8.

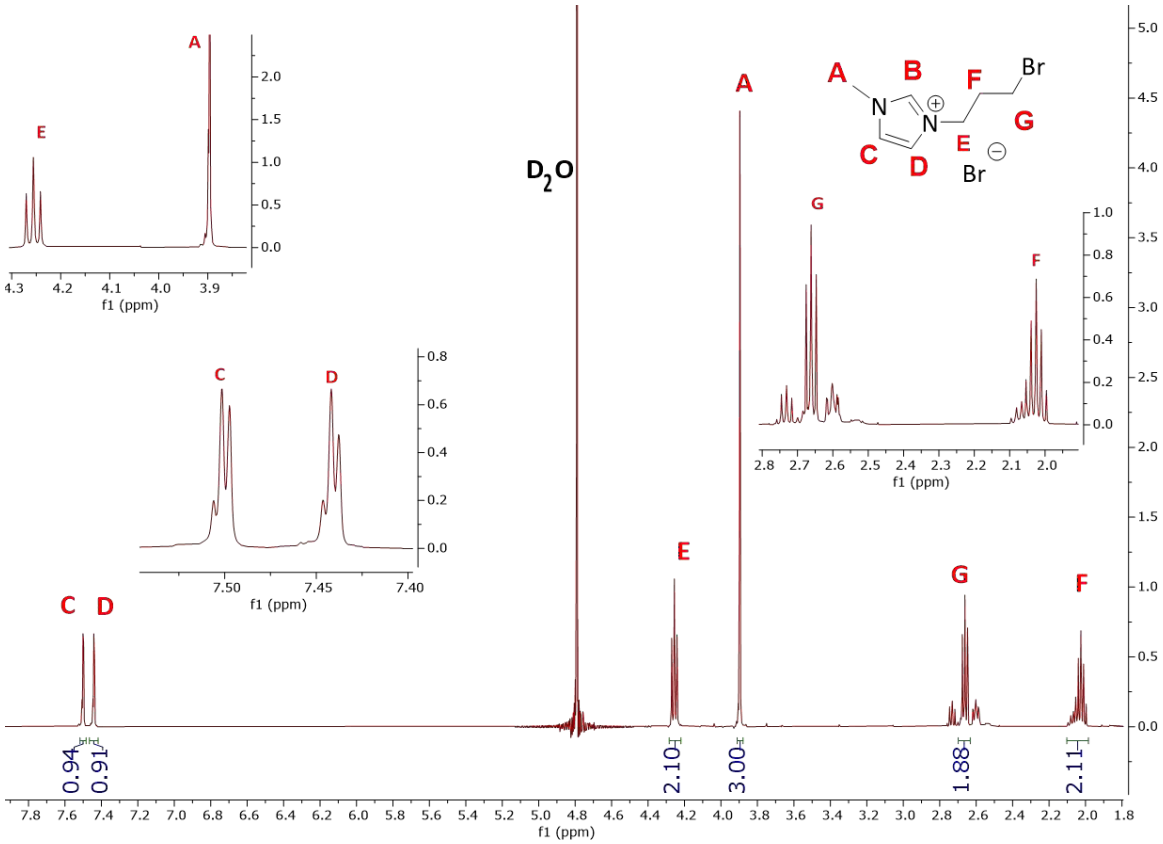

Figure 8: ^{1}H-NMR (D_2O) spectrum and the structure of compound 1-[PMIM-NH_2] [Br], after purification.

We were expecting eight signals based on the product structure as shown in Figure 8 and insects for every proton. We found two aromatic protons C and D, in the region 7-8 ppm, with doublet having an integration value of approximately one. There were no extra signals present in the aromatic region, proving the purification of compound 1 had occurred. Proton A was found as a singlet with an integration value of approximately three. The alkyl protons E, F, and G were found in the range of 2-5 ppm. Furthermore, they had integration values consistent with our expected values except for proton G, which was slightly low but close to characteristic integration value 2. Protons E and F showed proper triplet and multiplet (pentet) with an approximate integration of 2.10 and 2.18. Deuterated water as an NMR solvent gave more clear peaks with almost no unknown signals. However, we

were still missing two protons, B and H. We missed these proton signals because we were using a deuterated NMR solvent. In compound 1, we had two exchangeable protons, B and H, and as expected, they went under reaction with deuterated water and got converted into deuterium, which made them disappear from the ^{1}H-NMR spectrum.

We also tried DMSO-d6 as an NMR solvent after purifying compound 1, but we still observed several unidentified signals and the same unknown broad peak of approximately 3.8 ppm, as shown in Figure 6. We cannot identify these additional signals at this time. However, they are tentatively attributed to the reaction of amines with DMSO-d6 in the presence of oxygen.[27] After small-scale synthesis, we tried large-scale synthesis.

- **2.3 Large-scale synthesis of compounds 1 and 2**

After small-scale synthesis, one of our group members, Jeffery Palmer, performed a large-scale synthesis of amine-functionalized ionic liquid. For large-scale synthesis, after many experiments, we conclude that we can get rid of the ethanol as a solvent that we used for small-scale synthesis as we found more yield without having solvent in the reaction. So, for the large-scale synthesis of compound 1 (Figure 9), 1-methylimidazole (20.0 mL, 250 mmol) and 3-bromopropylamine hydrobromide (55.0 g, 250 mmol) were added to a 50 mL round bottom flask having a stir bar in it and placed in an oil bath. The solution appeared to be a semi-translucent yellow. The oil bath was heated to 100 °C with stirring at 300 rpm, and the solution was allowed to react for 26 hours. After the reaction, the solution became an opaque dark brown oil that quickly solidified at room temperature. In the purification process, we added 300 mL of water to the solution, and sodium hydroxide was added to make pH 10. The organic-soluble species were extracted by dichloromethane (three

extractions, 20 mL each), the water was evaporated, and the residue was washed three times with diethyl ether (50 mL each).

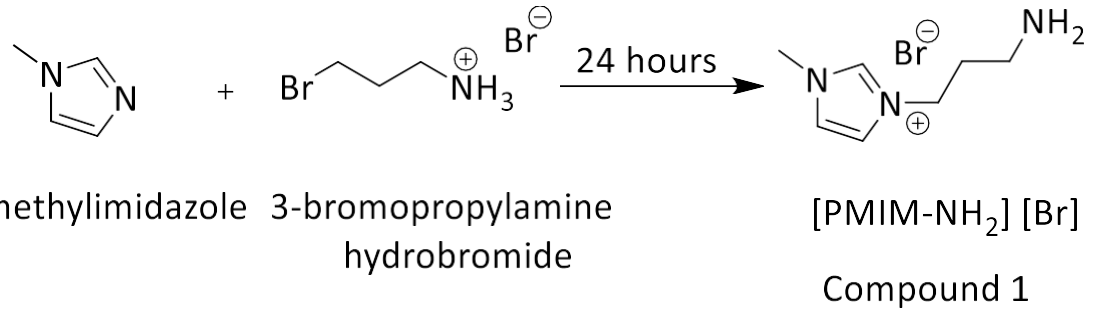

Figure 9: Reaction scheme for the large-scale synthesis of amine-functionalized imidazolium ionic liquid (compound 1) without solvent.

The product was dried under a vacuum oven at 70 °C overnight for 25 hours, leaving the dark brown semi-translucent product. The product, after purification, was then immediately used for compound 2 synthesis.

Compound 1 was reacted with lithium bis(trifluoromethanesulfonyl)imide ($LiTf_2N$) to replace bromide anion with the desired bistriflimide anion to synthesize propyl methyl imidazolium amine with bistriflimide (Tf_2N) anion ([PMIM-NH_2] [Tf_2N], Compound 2), as shown in Figure 10. For synthesis, the purified product obtained from the quaternization reaction was mixed with lithium bis(trifluoromethanesulfonyl)imide (57.4 g, 200 mmol) in 150 mL of water and allowed to stir for 20.5 hours. Here, we estimated the yield of compound 1 based on observations from previous experiments, and we used that estimate to gauge the amount of $LiTf_2N$ needed to synthesize compound 2. In the future, the yield of compound 1 should be determined and used to calculate the exact amount of $LiTf_2N$ needed to synthesize compound 2.

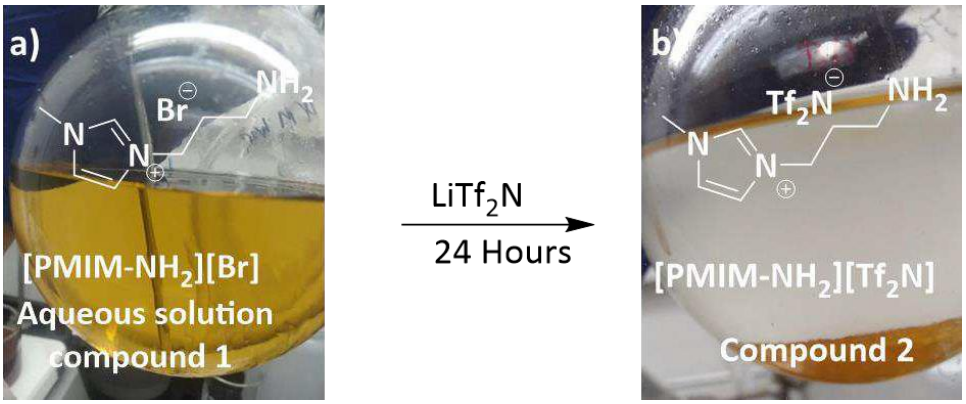

Figure 10: a) Picture of the aqueous solution of compound 1 at the start of the anion exchange reaction b) Picture of the two-phase mixture formed after the reaction.

The oily product, [PMIM-NH_2][Tf_2N], had separated from the water phase due to becoming more hydrophobic, suggesting the reaction was successful (Figure 10, b). For purification of compound 2, 200 mL of ethyl acetate was added to the solution. The water phase was removed from the reaction with the help of a separatory funnel. The product was then washed three more times with water (75 mL each) to remove any water-soluble components. The resulting amber liquid was then dried using a rotary evaporator and left overnight in a vacuum oven. The product was transferred to a tared bottle for long-term storage. After purification (Figure 11), the oil was weighed 56.10 g, with a percent yield of 74.3%.

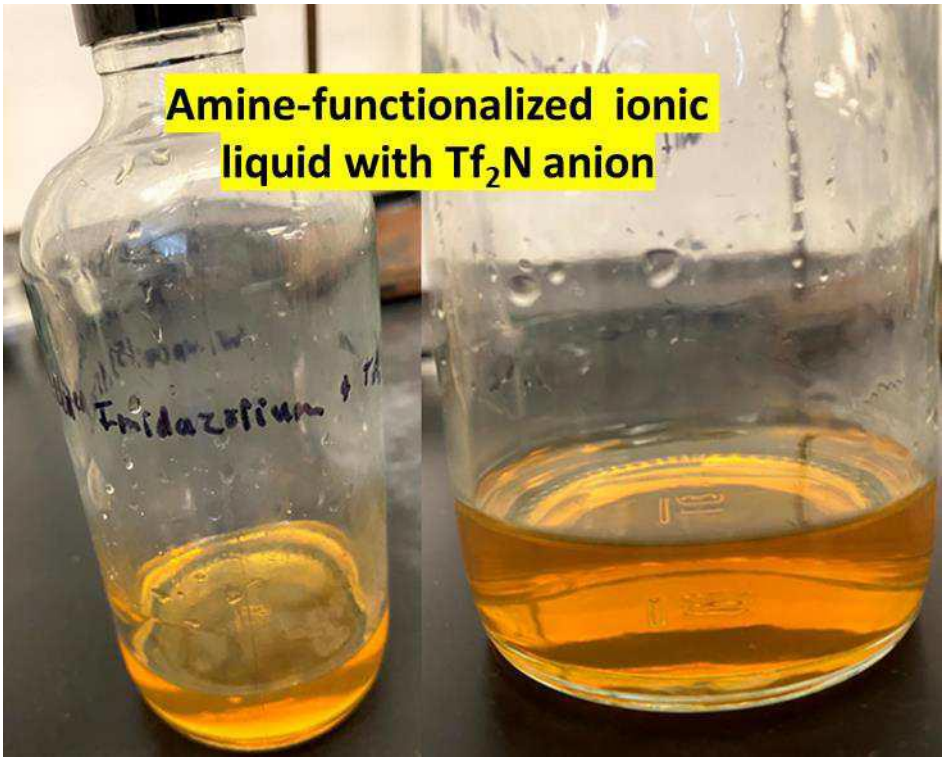

Figure 11: Amine functionalized product (compound 2) after large-scale synthesis.

Compound 2 was again purified before taking NMR. A 3 mL aliquot was taken from compound 2 (Figure 11) and dissolved in 5 mL of ethyl acetate, purified further using two 4 mL washes with water, and dried using a rotary evaporator. The NMR was taken to characterize compound 2 (Figure 12). We have seen a spectrum with almost no starting material or impurities for the small-scale synthesis of compound 1 when using D_2O as an NMR solvent, as shown in Figure 3.

The eight groups of hydrogens were counted based on the structure of the amine-functionalized ionic liquid as shown in figure 9, though only six signals are expected in the spectrum of compound 2 with D_2O solvent as protons B and H exchangeable protons. On the NMR spectrum (Figure 12), we got two aromatic protons C and D, from 7-10 ppm, and we got the expected doublet with the integration value of 1. The following signal was proton A, and we got the expected singlet with an integration value of 3.17. Alkyl protons

E and G were seen between 2-5 ppm with expected triplets with integration values of 2 and 2.12. Lastly, for proton F, we got a triplet with an integration value of 1.90. The extraneous peak around 4.7 ppm was due to water, and contamination signals in the chemical shift range of 1.0 - 3.6 ppm were found to be from unreacted 3-bromopropylamine hydrobromide. For further characterization of compound 2, we are going to use Carbon NMR spectrum and Mass spectrometry.

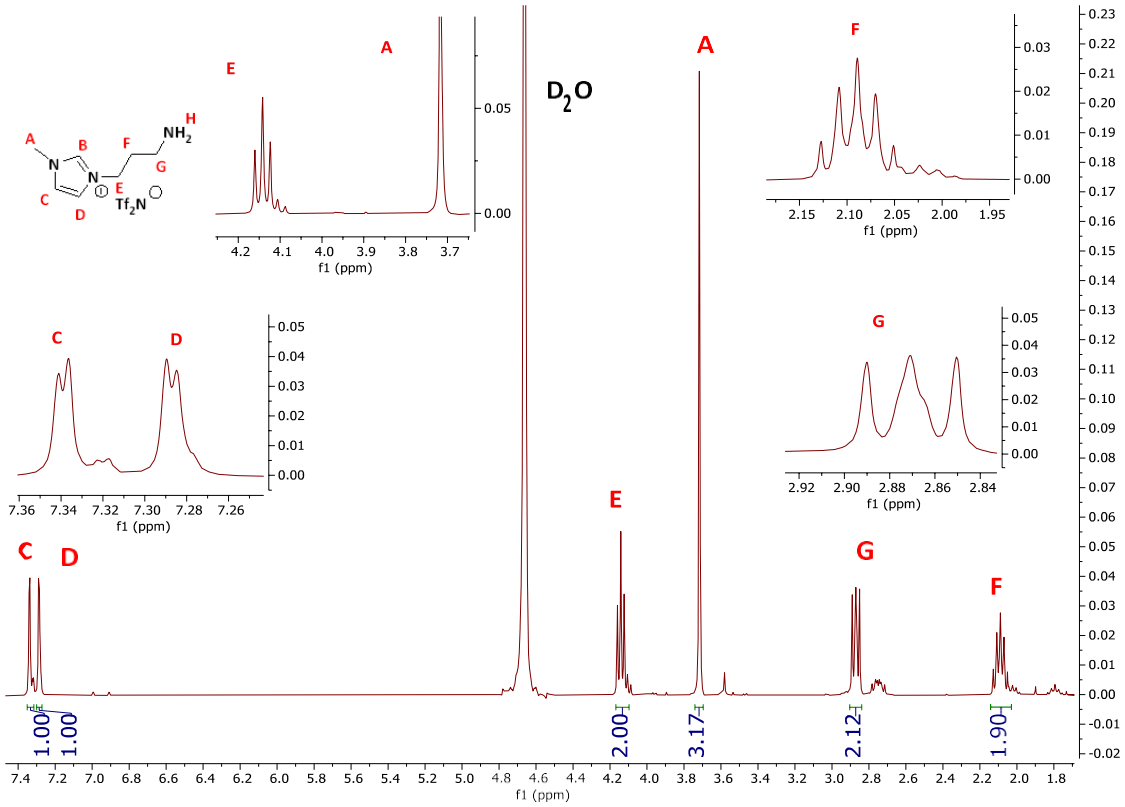

Figure 12: ^{1}H-NMR (D_2O) spectrum and the structure for large-scale synthesized compound 2-[PMIM-NH_2] [Tf_2N].

With the amine-functionalized ionic liquid in hand, we turned our attention to synthesizing thiol-functionalized ionic liquids discussed in chapter 3.

Chapter 3 - Synthesis of thiol-functionalized ionic liquids

The second functionalized ionic liquid that we want to synthesize for our project is a thiol-functionalized ionic liquid. The synthesis was similar to amine-functionalized ionic liquid synthesis, in which a quaternization reaction was followed by an ion-exchange reaction. We can synthesize thiol-functionalized ionic liquid by three different routes depending on the starting material used, as shown in Figure 13.

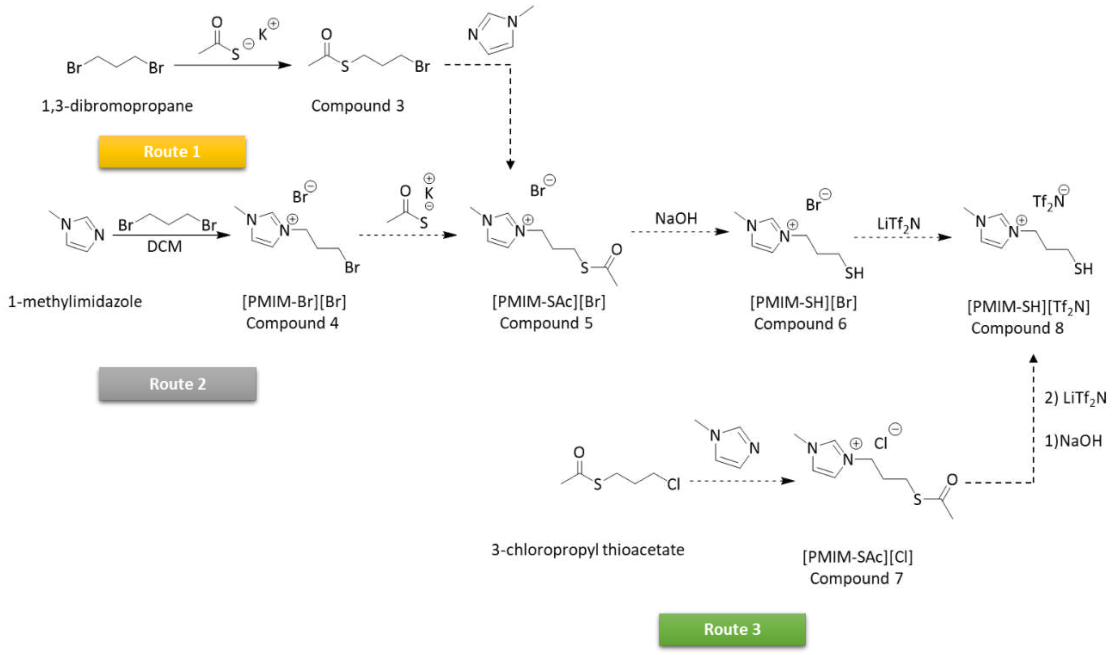

Figure 13: Different routes for the synthesis of thiol-functionalized ionic liquid. Routes 1, 2, and 3 are discussed in sections 3.3, 3.4, and 3.5, respectively.

3.1 Materials and Instrumentation

1-methylimidazole was purchased from Arcos Organics. 1,3-dibromopropane and potassium thioacetate were purchased from Alfa Aesar, Lithium bis(trifluoromethanesulfonyl)imide ($LiTf_2N$) was purchased from Tokyo Chemical Industry. Ethyl acetate and hexane were purchased from Sigma Aldrich. Deuterated dimethyl sulfoxide (DMSO-d6) and 3-chloropropyl thioacetate were purchased from

Oakwood Chemical. Deuterated water (D_2O) and deuterated chloroform were purchased from Aldrich Chemistry. Silica gel– grade 60 was purchased from Fisher Chemical. All the chemicals were used directly with no further purification. A JNM-ECZS 400 MHz nuclear magnetic resonance instrument (JEOL) was used to characterize the synthesized products, and NMR data were processed using MestReNova software.

3.2 Different routes for the synthesis of thiol-functionalized ionic liquid

We can make the thiol-functionalized ionic liquid in three distinct ways (Figure 13). All three routes involve the quaternization of methylimidazole. The main difference between the routes is where we performed the quaternization reaction. In route 1, the thioester (compound 3) is synthesized, followed by a quaternization reaction to obtain compound 5. In route 2, the quaternization reaction is first followed by a reaction with potassium thioacetate to get compound 5. In route 3, we found commercially available thioester to try for quaternization reaction, cutting down one reaction step.

3.3 Route 1 - Synthesis of thiol-functionalized ionic liquid

In route 1, the thiol-functionalized imidazolium ionic liquid synthesis was planned over three steps based on a previously reported method (Figure 13, Route 1).[28] We synthesized thioester first and performed a quaternization reaction followed by an ion-exchange step giving the desired product.

- **3.3.1 Synthesis of the compound 3 via route 1**

For the synthesis of compound 1, 1,3-dibromopropane (9.08 mL, 89.45 mmol) was taken in a round bottom flask, and potassium thioacetate (3.46 g, 30.29 mmol) was dissolved in ethanol (63 mL) by sonication for 25 minutes (Figure 14). The dissolved potassium

thioacetate was added dropwise to 1,3-dibromopropane; this addition took approximately 2.5 hours with no external heat.

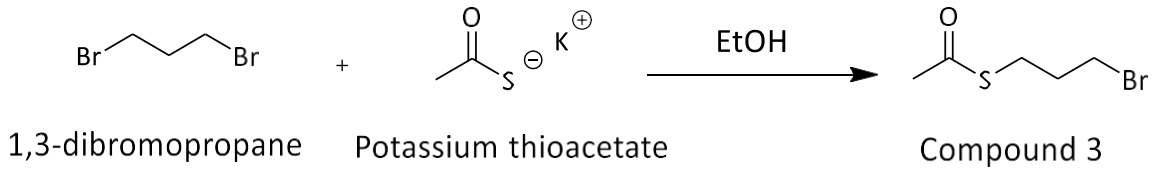

1,3-dibromopropane Potassium thioacetate Compound 3

Figure 14: Reaction scheme for the synthesis of compound 3 via route 1.

After dropwise addition, the thin-layer chromatography (TLC) technique was used to identify the eluent for column chromatography. There was no separation when we used 100% hexane as eluent for the TLC plate, whereas when we used 97% hexane and 3% ethyl acetate as eluent, there was separation on the TLC plate. Therefore, based on TLC observations, we decided to use 97% hexane and 3% ethyl acetate as eluent.

The mixture formed after dropwise addition was immediately filtered on cotton and rinsed with a small volume of ethyl acetate, and it took approximately 30 minutes. The solvent was evaporated at 65°C, stirring at 200 rpm for 1 hour, and after that, it was allowed to cool down at room temperature. Next, compound 3 was filtered through a dry-packed silica column. The column was washed with hexanes (90 – 100 mL), EtOAc/Hexanes (3:97, 100 mL), and TLC showed no product was obtained from these washes. Methanol (60 – 70 mL) was then used to collect the product from the column.

Methanol wash evaporated by a rotatory evaporator for 20 minutes giving the desired product based on NMR data (Figure 15). The practical yield of compound 3 was 0.57 grams, and the percent yield was 9.5 %.

- **3.3.2 Result and analysis of compound 3 synthesized via route 1**

For the characterization of compound 3, proton nuclear magnetic resonance spectroscopy was used. The NMR data was first collected by deuterated water followed by deuterated

dimethyl sulfoxide as NMR solvent. Based on the structure of compound 3 (Figure 15), we were expecting four signals. We found four expected signals, A, B, C, and D, with some unknown signals. We found two signals for protons B and D from 2-4 ppm with an expected triplet with the integration value of approximately two. The integration values were below expected for protons B and D, and the signals were with some impurities from starting materials.

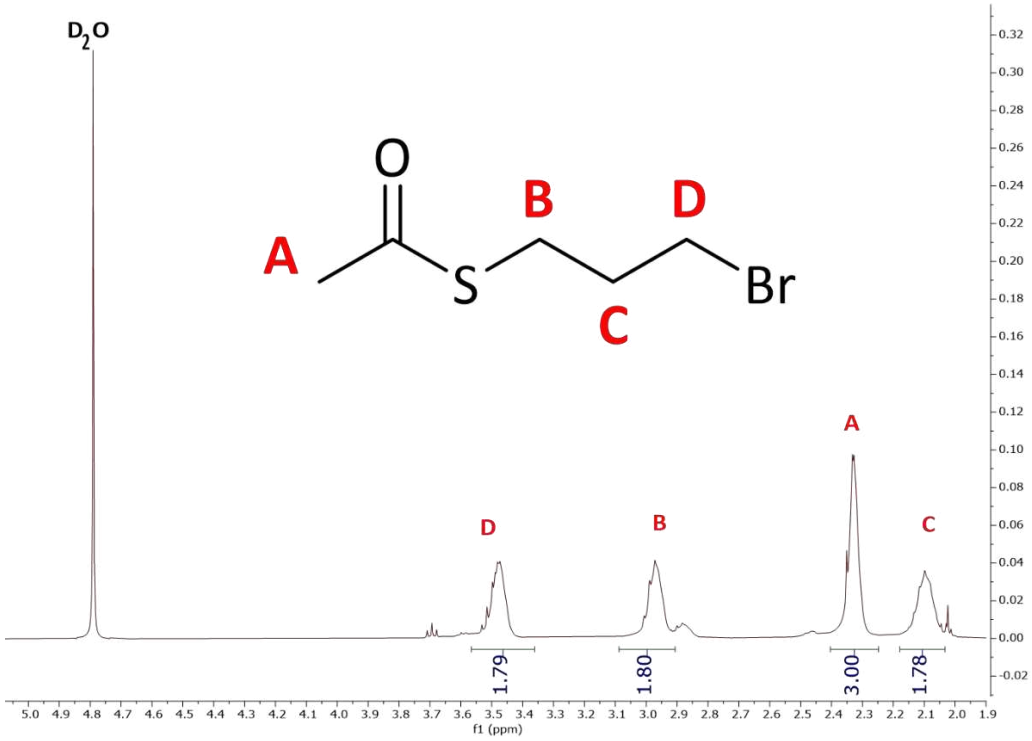

Figure 15: ^{1}H-NMR (D_2O) spectrum compound 3.

Protons A and C were expected and found to be multiplet (pentet) and singlet with integration values of 2 and 3. The integration value of proton A was close to expected, but proton C had a lower integration value on NMR data. All signals were found to be broad, and it was likely because of poor solubility in water. So, we decided to try deuterated dimethyl sulfoxide as an NMR solvent as it was previously used for amine-functionalized ionic liquid synthesis and gave good spectrum signals.

Deuterated dimethyl sulfoxide used as an NMR solvent for compound 3; as shown in Figure 16, all four expected protons D, B, A, and C found triplet, triplet, singlet, and multiplet (pentet) signals. Adjacent to proton B, we had small triplet signals in the range of 2.8 – 2.9 ppm from starting material, indicating that the product signals were shifted from the starting materials. For proton A, the integration value was high by 0.48 as there was a shoulder on the peak along with the expected signal, and it must be from starting material. There were still a few impurities in the spectrum, and they are primarily from starting materials.

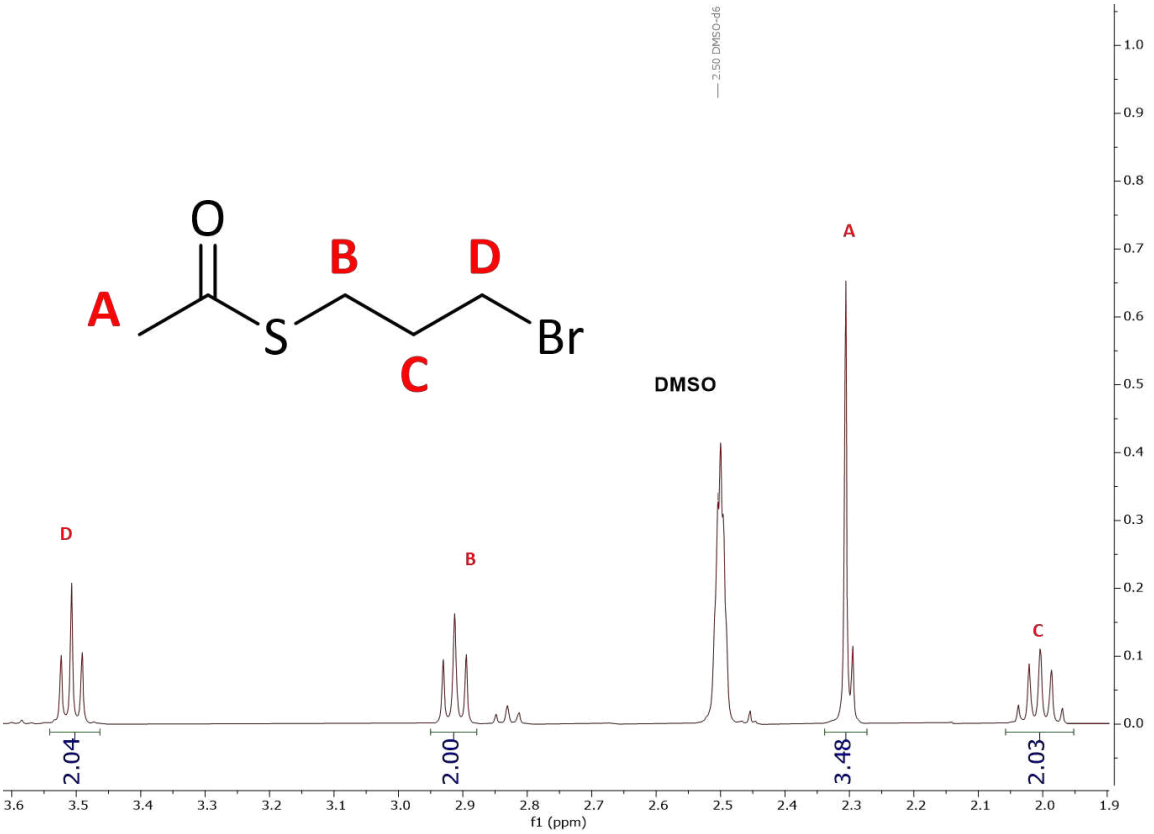

Figure 16: ^{1}H-NMR (DMSO-d6) spectrum compound 3.

Overall, based on both NMR data (Figure 15 and Figure 16), we concluded that we got the expected compound 3 with few impurities and low practical yield, but we can try the synthesis of compound 5.

- **3.3.3 Synthesis of the compound 5 [PMIM-SAc] [Br] via route 1**

The next step in route 1 was the quaternization reaction step, in which 1-methylimidazole was quaternized by compound 3. In this quaternization reaction, lone pair on nitrogen atom from 1-methylImidazole attacked the alpha carbon of compound 3 in a nucleophilic substitution reaction (S_N2) with bromide acting as leaving group and gave compound 5 that is propyl methyl imidazolium thioacetate with bromide anion abbreviated as [PMIM-SAc] [Br].

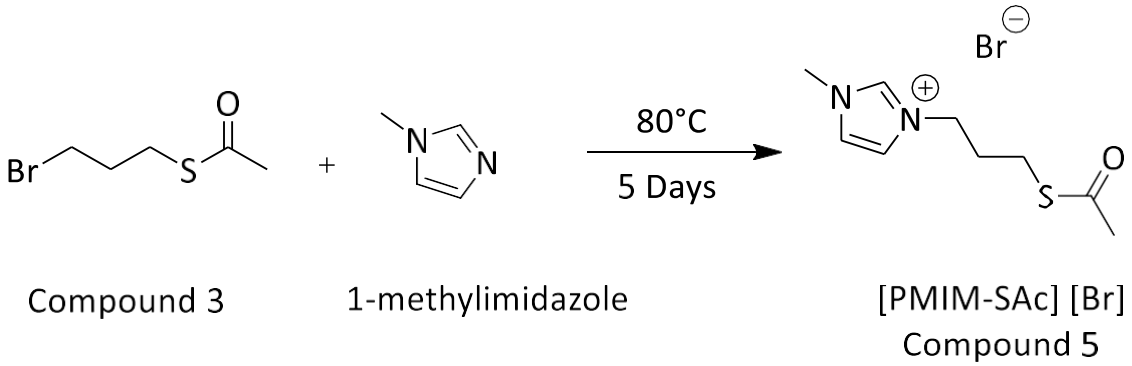

Figure 17: Reaction scheme for the synthesis of compound 5 via route 1.

For the synthesis of compound 5 (Figure 17), compound 3 (0.29 g, 1.038 mmol) and 1-methylimidazole (0.11 mL, 1.37 mmol) were added in a round-bottom flask, heated to 80°C, and agitated for five days. Next, 10 mL hexane was used to wash the product, and hexane was evaporated under reduced pressure at 50^0C with stirring at 200 rpm for 22 minutes, leaving a greenish solid. Compound 5 was characterized by using proton nuclear magnetic resonance spectroscopy and DMSO as solvent. We were expecting eight signals based on the structure of compound 5 (Figure 18). The NMR was a little messy with unexpected signals. We found three expected aromatic signals B, C, and D in the aromatic region 7-9 ppm with expected integration values. However, we can also see three other signals from our starting material, 1-methylimidazole, as it should give the three similar

aromatic signals. Alkyl protons E, G, and F were found on the spectrum from 1.5-5 ppm with an expected triplet, triplet, and multiplet (pentet) and the approximately expected integration. Another essential indication was for proton H, and we were missing this signal from the spectrum. Purification of compound 5 may help us observe proton H.

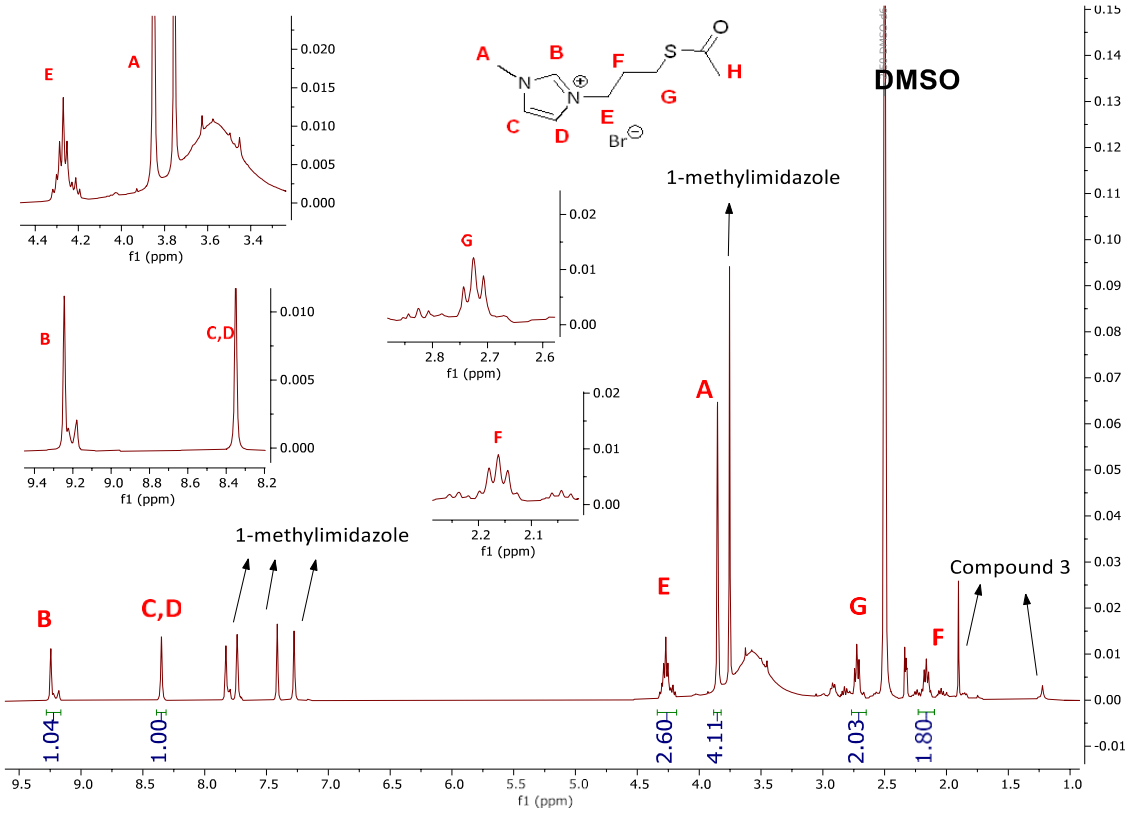

Figure 18: ^{1}H-NMR (DMSO-d6) spectrum of compound 5.

We can also see a broad peak at 3.8 ppm having A proton signal from methylimidazole. We are still unsure about the broad peak at 3.8 ppm, though we have seen the same broad peak whenever we have quaternized product and DMSO-d6 as NMR solvent. For the source of impurities in compound 5, we took the NMR of starting materials in the same NMR solvent as compound 5 and stacked their NMR plots on MestReNova software, as shown in Figure 19.

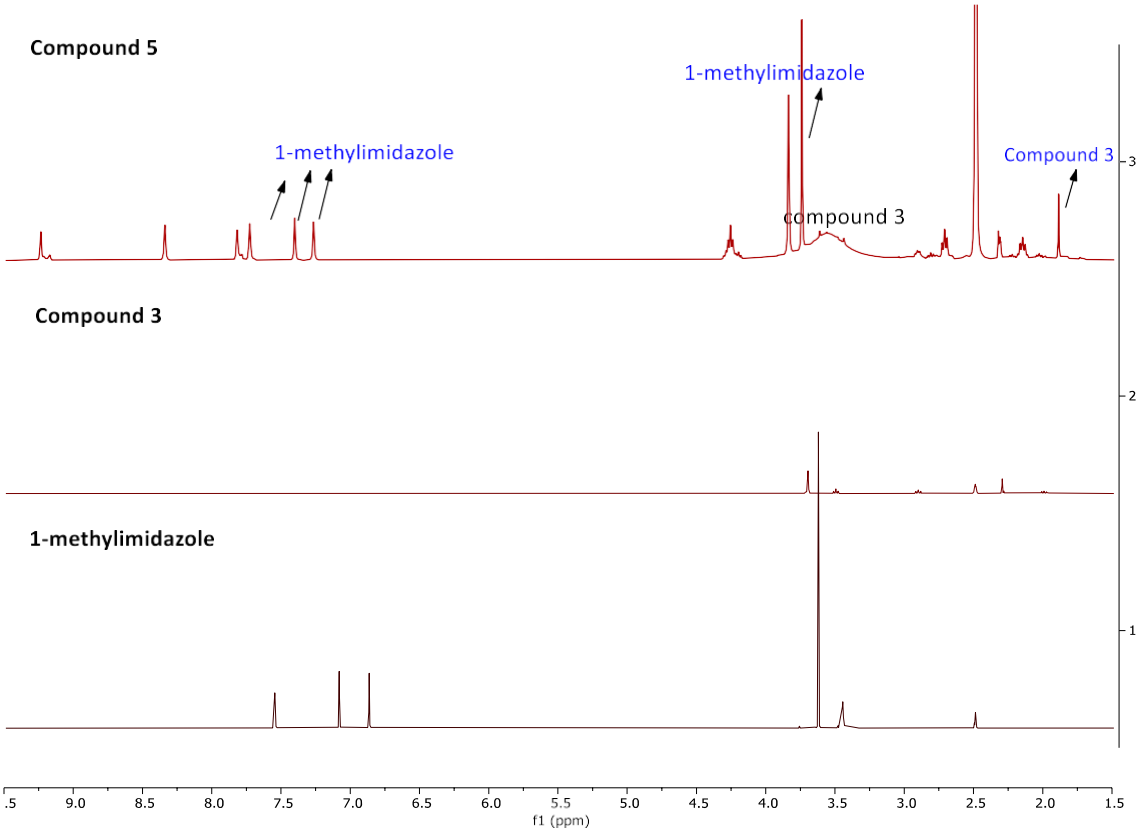

Figure 19: Stacked ^{1}H-NMR (DMSO-d6) spectrums of reactants and compound 5.

After stacking the NMR spectra of the starting materials and compound 5, we found that three extra aromatic signals in the 7–8 ppm and peak at 3.6 ppm were likely from the 1-methylimidazole. These additional signals in the aromatic region provide evidence for forming the new bond for the quaternization reaction. The small set of unexpected signals from 1.5 – 2 ppm looks like from compound 3. Based on the NMR data (Figures 18 and 19), it was found that there was some starting material available as impurities, so compound 5 needs to be purified.

For the purification process, it was essential to find the proper solvent. To find out about three extra aromatic signals in the 7–8 ppm and peak at 3.6 ppm, we planned a new experiment in which we will add 1-methylimidazole to the NMR sample of compound 5. If we have 1-methylimidazole as impurities, a new NMR will give us stronger aromatic

signals and indicate impurities from 1-methylimidazole. Overall, based on three extra signals in the aromatic region (Figures 18 and 19), provide evidence for forming the new bond for the quaternization reaction; however, we were missing H proton from thioacetate on the spectrum of compound 5 is still unclear. We are working on this approach and trying to purify compound 5, and if we get purified and desire product, we will try further steps.

3.4 Route 2 - Synthesis of thiol-functionalized ionic liquids

In route 2, the 1-methylimidazole was quaternized by reacting with the 1,3-dibromopropane, and the remaining primary bromide was converted to the corresponding thiol using potassium thioacetate, then treated with a highly alkaline solution. Finally, by metathesis, the resulting imidazolium bromide with $LiTf_2N$, a thiol-functionalized ionic liquid with the desired anion, will be obtained (Figure 20).

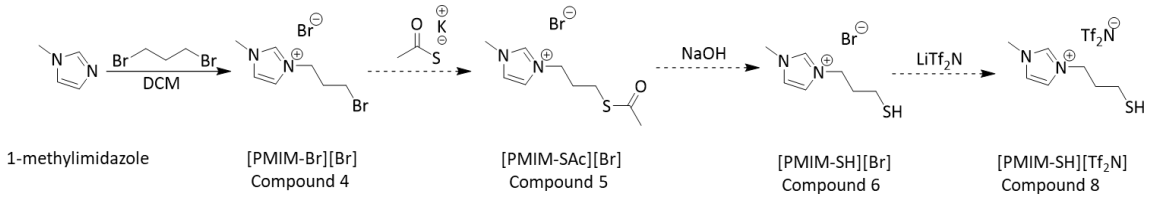

Figure 20: Synthesis of thiol-functionalized imidazolium ionic liquid via route 2.

- **3.4.1 Synthesis of compound 4 [PMIM-Br] [Br] via route 2**

In this synthesis route for ionic liquid with a thiol functional group, a modified version of the reaction mechanism outlined by Richard et al was used, as shown in Figure 21.[29] For synthesis, 1-methylimidazole (2.09 mL, 6.02 mmol), 1,3-dibromopropane (20.5 g, 98.50 mmol) and 10 mL of dichloromethane were added to a 50 mL round bottom flask with a stir bar and placed in an oil bath. The oil bath was heated to 40°C, and the reaction mixture was stirred at 300 rpm for 12 hours. Then, the solvent was removed under reduced pressure, and the residue was washed thoroughly with hexane to remove excess dibromopropane.

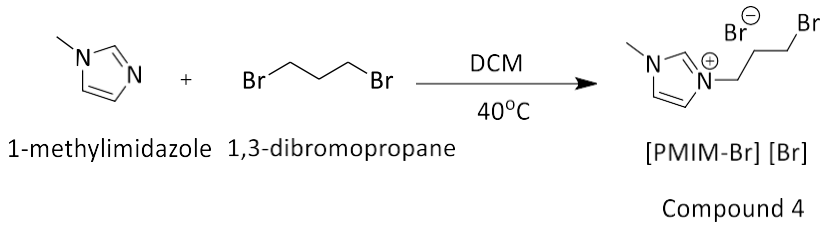

Figure 21: Reaction scheme for the synthesis of compound 4 [PMIM-Br] [Br], route 2.

- **3.4.2. Result and analysis of compound 4 [PMIM-Br] [Br]**

For characterization of compound 4, ^{1}H-NMR was used, and deuterated chloroform was used as an NMR solvent. Based on the structure of compound 4 (Figure 22), we were expecting seven signals. Aromatic protons B, C, and D, were seen in the range of 7-10 ppm with integration values of approximately one, two, and two, respectively. The next proton for compound 4 was proton A, which should be a singlet with a relative integration value of roughly three; here, we saw a singlet that integrates for 3.22 on the spectrum. The alkyl protons E, F, and G were seen in the range of 2 - 5 ppm. Moreover, the protons E and G found triplets and proton F with multiplet (pentet) with approximate integration of two, and these integration values consistent with expected values.

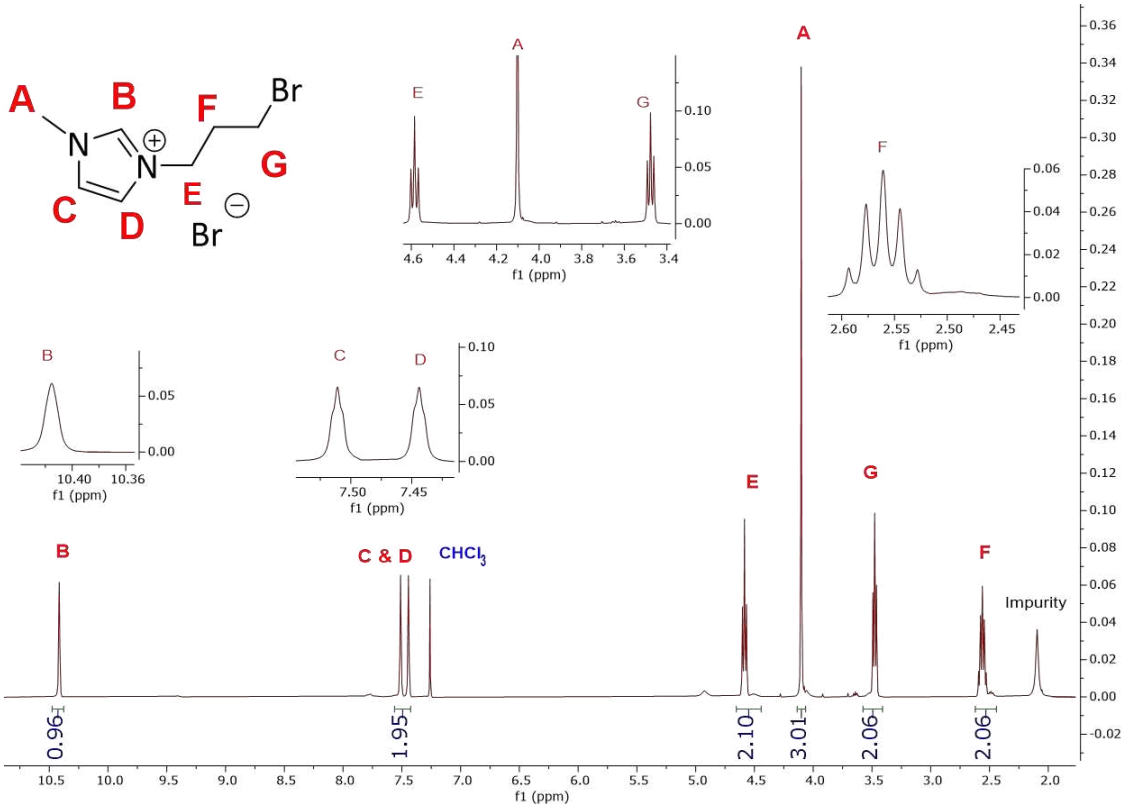

Figure 22: ^{1}H-NMR ($CDCl_3$) spectrum of compound 4 [PMIM-Br] [Br].

The unknown signals may be from starting materials methylimidazole and 1,3-dibromopropane. However, after stacking the reactants and compound 4, it made clear that the additional signals were from unreactive starting materials. For the subsequent trial of this reaction, along with ^{1}H-NMR we will use C-NMR and mass spectrometry for further characterization.

- **3.4.3 Synthesis of compound 5 [PMIM-SAc] [Br] via route 2**

In this, compound 4 was reacted with potassium thioacetate, and bromide on the alkyl chain is replaced by thioacetate (Compound 5), as shown in figure 25. We synthesized compound 5 many times, but it always gave NMR data with unknown signals. We are still working to synthesize compound 5 by route 2. We tried different potassium thioacetate concentrations to synthesize compound 5, longer and monitored reactions, different temperature conditions. NMR data after all these trials have desired product on small scale or approximately half of compound 4 converted into compound 5 and have more impurities and all these hurdles lead us to find new chemicals that cut down reaction steps for thiol synthesis.

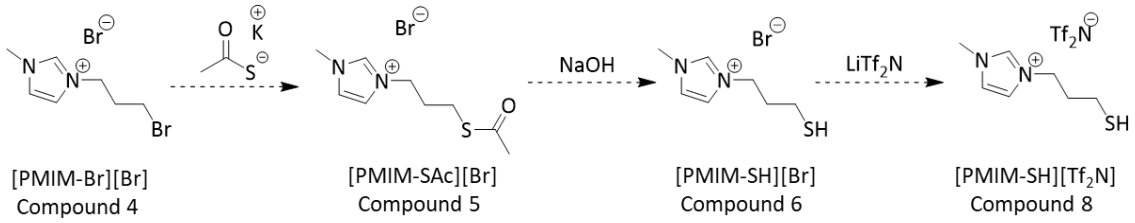

Figure 23: Future synthesis steps for thiol-functionalized imidazolium ionic liquid via route 2.

Once we replace the bromide with thioacetate for compound 5, we will replace thioacetate with thiol, and lastly, the bromide anion will be replaced by bistriflimide (Tf_2N), as shown in Figure 23.

3.5. Route 3 - Synthesis of thiol-functionalized ionic liquid

After using two different starting materials for route one and route two, compounds 3 and 4 were synthesized with impurities with a low yield, and it was difficult to purify them. So, instead of repeatedly synthesizing compounds 3 and 4, we can use commercially available new chemicals to save time, chemical cost and eliminate impurities. We decided to use commercially available 3-chloropropyl thioacetate as a starting material that cut down one synthesis step. Route 3 works similar to the amine-functionalized ionic liquid synthesis. In the first step, 1-methylimidazole will be quaternized by reacting with the 3-chloropropyl thioacetate following metathesis of the resulting imidazolium chloride by reacting with lithium bis(trifluoromethanesulfonyl)imide ($LiTf_2N$) and will yield thiol-functionalized ionic liquids with the desired anion as shown in the below figure 24.

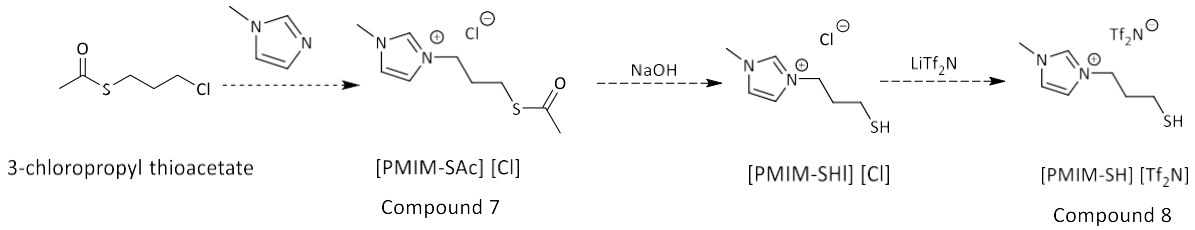

Figure 24: Proposed synthesis for thiol-functionalized imidazolium ionic liquid with new chemical, route 3.

Chapter 4 – Conclusion and future directions

So far, we synthesized and identified amine-functionalized ionic liquid [PMIM-NH_2][Tf_2N]. The method (Figure 4) used and has given a significant yield of 74.3%. It is one of the targeted ionic liquids from desire amine, and thiol functionalized ionic liquids.

The nanoparticle synthesis using traditional ligands has been optimized for efficiency by our group, allowing for shape control of the nanoparticles on a small scale. Finally, these methods will be replicated for shape control by using synthesized ionic liquids.

We ordered a new chemical and have preliminary results for some steps of the thiol-functionalized ionic liquid synthesis, though the targeted ionic liquid (Compound 8) has not yet been obtained. From here, future steps are first to confirm whether shape control of platinum nanoparticles can be achieved with the amine-functionalized ionic liquid. Then, the synthesis method can be optimized for the new materials while the thiol-functionalized ionic liquid is developed.

Once both ionic liquids are synthesized, and a nanoparticle synthesis method is identified, they will be used to synthesize platinum cobalt nanoparticles, and then transmission electron microscopy (TEM) will be used to confirm whether shape control is achieved or not. Finally, once the ideal shape is achieved, they will be tested for hydrogenation reaction to compare their rates of catalytic conversion to platinum nanoparticles made using traditional ligands.

BIBLIOGRAPHY

(1) Naumann, G.; Alfieri, L.; Wyser, K.; Mentaschi, L.; Betts, R. A.; Carrao, H.; Spinoni, J.; Vogt, J.; Feyen, L. Global Changes in Drought Conditions Under Different Levels of Warming. *Geophys. Res. Lett.* **2018**, *45* (7), 3285–3296.

(2) The hard truths of climate change — by the numbers. Nature, **2019**, vol 573, 324-327.

(3) Li, B.; Duan, Y.; Luebke, D.; Morreale, B. Advances in CO2 Capture Technology: A Patent Review. *Appl. Energy* **2013**, *102*, 1439–1447.

(4) Spigarelli, B. P.; Kawatra, S. K. Opportunities and Challenges in Carbon Dioxide Capture. *J. CO2 Util.* **2013**, *1*, 69–87.

(5) Zhan, H.; Li, F.; Gao, P.; Zhao, N.; Xiao, F.; Wei, W.; Zhong, L.; Sun, Y. Methanol Synthesis from CO2 Hydrogenation over La–M–Cu–Zn–O (M = Y, Ce, Mg, Zr) Catalysts Derived from Perovskite-Type Precursors. *J. Power Sources* **2014**, *251*, 113–121.

(6) Sun, Y.; Hu, H.; Wang, Y.; Gao, J.; Tang, Y.; Wan, P.; Hu, Q.; Lv, J.; Zhang, T.; Yang, X. J. In Situ Hydrogenation of CO2 by Al/Fe and Zn/Cu Alloy Catalysts under Mild Conditions. *Chem. Eng. Technol.* **2019**, *42* (6), 1223–1231.

(7) Introduction to Catalysis. In *Concepts of Modern Catalysis and Kinetics*; John Wiley & Sons, Ltd, 2003; pp 1–21.

(8) Ye, R.-P.; Ding, J.; Gong, W.; Argyle, M. D.; Zhong, Q.; Wang, Y.; Russell, C. K.; Xu, Z.; Russell, A. G.; Li, Q.; Fan, M.; Yao, Y.-G. CO 2 Hydrogenation to High-Value Products via Heterogeneous Catalysis. *Nat. Commun.* **2019**, *10* (1), 5698.

(9) Qadir, M. I.; Weilhard, A.; Fernandes, J. A.; de Pedro, I.; Vieira, B. J. C.; Waerenborgh, J. C.; Dupont, J. Selective Carbon Dioxide Hydrogenation Driven by Ferromagnetic RuFe Nanoparticles in Ionic Liquids. *ACS Catal.* **2018**, *8* (2), 1621–1627.

(10) Khan, I.; Saeed, K.; Khan, I. Nanoparticles: Properties, Applications and Toxicities. *Arab. J. Chem.* **2019**, *12* (7), 908–931.

(11) Feynman, R. P. There's Plenty of Room at the Bottom. *Eng. Sci.* **1960**, *23* (5), 22–36.

(12) Sandhu, A. Who Invented Nano? *Nat. Nanotechnol.* **2006**, *1*, 87–87.

(13) Drexler, K. E. Engines of Creation : The Coming Era of Nanotechnology. 10.

(14) Benelmekki, M. *Designing Hybrid Nanoparticles*; Morgan & Claypool Publishers, **2015**.

(15) Pokropivny, V. V.; Skorokhod, V. V. Classification of Nanostructures by Dimensionality and Concept of Surface Forms Engineering in Nanomaterial Science. *Mater. Sci. Eng. C* **2007**, *27* (5), 990–993.

(16) Size-Controlled Synthesis of Gold Nanoparticles from Bulk Gold Substrates by Sonoelectrochemical Methods | The Journal of Physical Chemistry B

(17) Xiong, Y.; Xia, Y. Shape-Controlled Synthesis of Metal Nanostructures: The Case of Palladium. *Adv. Mater.* **2007**, *19* (20), 3385–3391.

(18) Lu, X.; Rycenga, M.; Skrabalak, S. E.; Wiley, B.; Xia, Y. Chemical Synthesis of Novel Plasmonic Nanoparticles. *Annu. Rev. Phys. Chem.* **2009**, *60* (1), 167–192.

(19) Mohamed, R. M.; McKinney, D. L.; Sigmund, W. M. Enhanced Nanocatalysts. *Mater. Sci. Eng. R Rep.* **2012**, *73* (1), 1–13.

(20) Li, C.; Liu, T.; He, T.; Ni, B.; Yuan, Q.; Wang, X. Composition-Driven Shape Evolution to Cu-Rich PtCu Octahedral Alloy Nanocrystals as Superior Bifunctional Catalysts for Methanol Oxidation and Oxygen Reduction Reaction. *Nanoscale* **2018**, *10* (10), 4670–4674.

(21) Yamada, L. K.; da Silva, A. G. M.; Rodrigues, T. S.; Haigh, S. J.; Camargo, P. H. C. Bimetallic Au@Pd-Au Tadpole-Shaped Asymmetric Nanostructures by a Combination of Precursor Reduction and Ostwald Ripening. *ChemNanoMat* **2016**, *2* (6), 509–514.

(22) Bandarenka, A. S.; Koper, M. T. M. Structural and Electronic Effects in Heterogeneous Electrocatalysis: Toward a Rational Design of Electrocatalysts. *J. Catal.* **2013**, *308*, 11–24.

(23) Shin, C.; Park, T. E.; Park, C.; Kwon, S. J. Observation of Single Pt Nanoparticle Collisions: Enhanced Electrocatalytic Activity on a Pd Ultramicroelectrode. *ChemPhysChem* **2016**, *17* (11), 1637–1641.

(24) Bratlie, K. M.; Lee, H.; Komvopoulos, K.; Yang, P.; Somorjai, G. A. Platinum Nanoparticle Shape Effects on Benzene Hydrogenation Selectivity. *Nano Lett.* **2007**, *7* (10), 3097–3101.

(25) Khan, M. U.; Wang, L.; Liu, Z.; Gao, Z.; Wang, S.; Li, H.; Zhang, W.; Wang, M.; Wang, Z.; Ma, C.; Zeng, J. Pt_3Co Octapods as Superior Catalysts of CO_2 Hydrogenation. *Angew. Chem. Int. Ed.* **2016**, *55* (33), 9548–9552.

(26) Bates, E. D.; Mayton, R. D.; Ntai, I.; Davis, J. H. CO_2 Capture by a Task-Specific Ionic Liquid. *J. Am. Chem. Soc.* **2002**, *124* (6), 926–927.

(27) Lin, M.; Wang, Z.; Fang, H.; Liu, L.; Yin, H.; Yan, C.-H.; Fu, X. Metal-Free Aerobic Oxidative Coupling of Amines in Dimethyl Sulfoxide via a Radical Pathway. *RSC Adv.* **2016**, *6* (13), 10861–10864.

(28) Mirjafari, A.; O'Brien, R. A.; West, K. N.; Davis, J. H. Synthesis of New Lipid-Inspired Ionic Liquids by Thiol-Ene Chemistry: Profound Solvent Effect on Reaction Pathway. *Chem. – Eur. J.* **2014**, *20* (25), 7576–7580.

(29) Gondosiswanto, R.; Gunawan, C. A.; Hibbert, D. B.; Harper, J. B.; Zhao, C. Microcontact Printing of Thiol-Functionalized Ionic Liquid Microarrays for "Membrane-Less" and "Spill-Less" Gas Sensors. *ACS Appl. Mater. Interfaces* **2016**, *8* (45), 31368–31374.